WAKE FIELD ACCELERATION

W. Bialowons, H.D. Bremer, F.-J. Decker, M. v. Hartrott,
H.C. Lewin, G.-A. Voss, T. Weiland, P. Wilhelm,
Xiao Chengde * and K. Yokoya †

Deutsches Elektronen-Synchrotron DESY
Notkestraße 85, 2000 Hamburg 52, West Germany

June 26, 1986

Abstract

We are investigating the possibility of accelerating particles with high gradients in a "Wake Field Transformer" [1,2]. The progress of this experiment will be described. The developement of the high current hollow beam electron gun was continued. In the conventional linac, the hollow beam was accelarated to about 6 MeV. Beam monitors came into operation, two gap monitors, two fluorescent monitors and a Čerenkov monitor. Calculations with the computer code WAKTRACK[3] gave the final details for the high energy section of the accelerator that will be installed during 1986.

INTRODUCTION

Circular accelerators for electrons are operating very successfully in the GeV range. As the synchrotron radiation increases with the fourth power of the energy, linear accelerators become attractive at very high energies, above 100 GeV. In the TeV region they are the only feasible choice.

To become achievable with respect to cost, they have to operate with high acceleration gradients. The total length of a linac is given approximately by

$$L \sim \frac{\text{center of mass energy}}{\text{accelerating gradient}}.$$

The common technology allows gradients up to 17 MeV/m [4], with superconductive cavities one reaches up to 20 MeV/m [5]. Laser accelerators [6], plasma accelerators or wakefield accelerators [9,10] promise much higher gradients (about 1 order of magnitude). Several methods have been discussed [6,7,8]. The DESY Wake Field Transformer experiment is carried out in order to recognize the inherent physical and technical problems in more detail and possibly to overcome them. As the principle has been described in detail elsewhere[1,2], we only recall the basics: A driving beam with high charge ($\approx 1\mu C$) passes the "Wake Field Transformer" (WFT), where it excites wake fields that lead to deceleration. By proper shaping of the WFT, the wave packet is subsequently spatially focussed. Thus the field strength increases proportionally to the inverse of the square root of the volume containing the wake fields. A second beam with lower charge ($\approx 0.01\mu C$) passes the transformer with a suitable delay and experiences a much greater acceleration than the deceleration of the driving beam.

Among different geometrical arrangements of the driving and driven beam[1,2], a hollow beam driving a thin beam on its center may be achieved most easily. Furthermore for this case the calculated magnitude of the transformation ratio is 10, which is large compared to other geomteries. Assuming a total charge of $1\mu C$ and a bunch length of 5 mm, we find values for the accelerating gradient above 100 MeV/m for the inner beam.

In the experiment (fig. 1), a laser driven gun produces a high current (1 kA, 150 keV) hollow ring beam of 10 cm diameter. In the prebuncher the hollow beam is bunched to a length of about 5 cm. The following linac consists of four 3-cell-cavities (500 MHz) powered by a 1 MW klystron. At the end of the linac, the bunch has a length of about 3 cm (rms) and an energy of 8 MeV. The whole equipment is put into a solenoid guiding field of 0.2 T. The final longitudinal

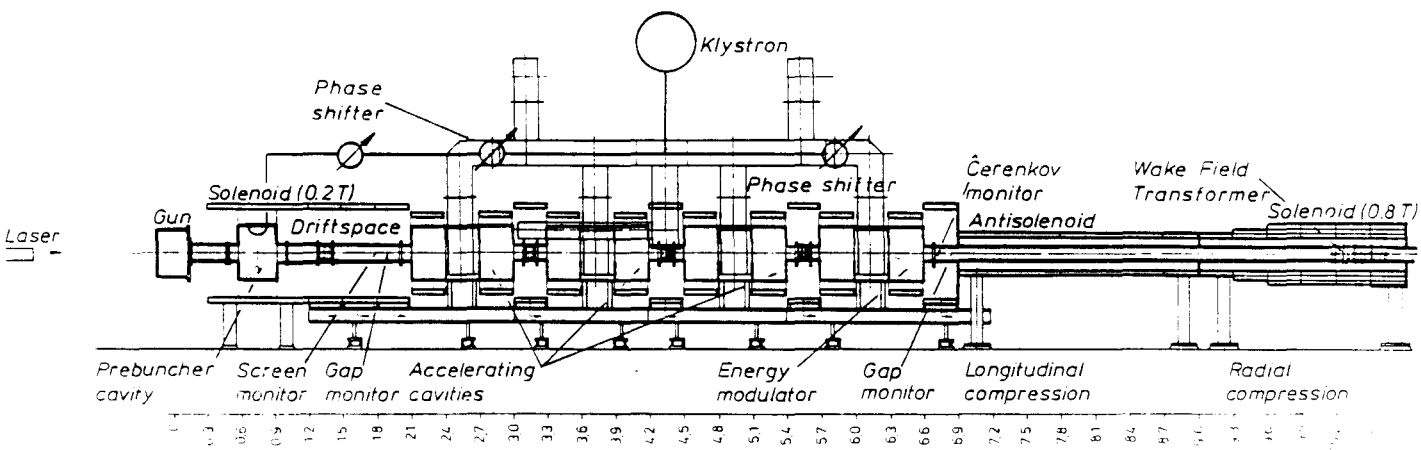

Fig. 1. *Overall layout of the Wake Field Transformer experiment at DESY shown from left to right: The infrared light beam produced by a Q-switched Nd-Yag laser (peak power > 100 MW) is focused on a ring shaped tantalum cathode. The emitted thermionic- and photoelectrons are extracted by a voltage of about 100 kV and guided by solenoid fields of 0.2 T into the linac. First the hollow beam becomes compressed longitudinally in a prebuncher. Then four 3-cell cavities (500 MHz) accelerate it to 8 MeV. A pulsed klystron (peak power 1 MW) feeds the cavities. In the antisolenoid further longitudinal compression is achieved. By increased solenoidal fields at the end radial compression takes place too. After that the electron ring enters the actual Wake Field Transformer, consisting of 80 cylindrical cells arranged one after another. For monitoring and adjustment of the ring beam, several beam monitors have been set up.*

*On leave from Tsinghua University, Beijing, People's Republik of China

†On leave from KEK National Laboratory for High Energy Physics, Japan

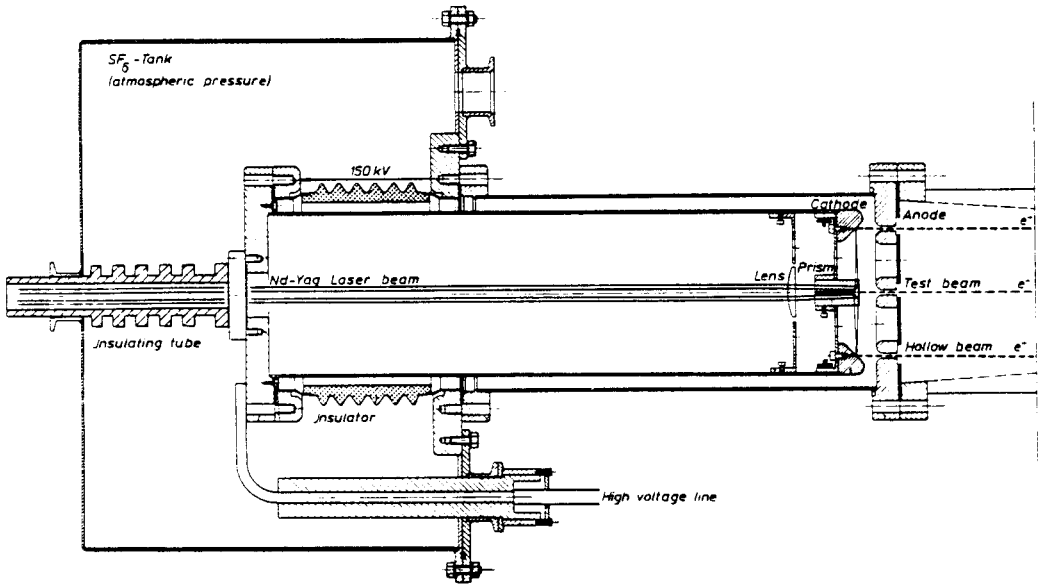

Fig. 2. *Cross section of the laser driven hollow beam gun. The infrared laser light is focussed on a ring at the tantalum cathode. The optical train consists of a viewing port, a focussing lens and a conical mirror. The conical mirror is a quartz cylinder with a polished inverse cone at the top, making use of the total reflection at the glass vacuum surface. The emission mechanism is explained by the generalized Richardson effect (pure thermionic effect and thermionic supported multiphotoneffect). The emitted electrons are extracted by a high voltage and guided by a solenoid field through a slot hole in the anode. In order to increase the break down voltage the insulating ceramic is surrounded by SF_6-gas at atmospheric pressure. The optical train is separated from the gas by an insulating tube.*

compression is achieved in the high energy buncher, after which the ring beam is fed into the Wake Field Transformer.

So far, the experimental set up has been installed up to the end of the linac.

THE GUN

Fig.2 shows the design of the gun. An infrared light pulse of a Nd-YAG laser, consisting of a 3 ns main pulse with two side maxima, is focused on a ring at the cathode. There electrons are extracted from the metal via heating and photo effect [10]. These are accelerated by the high voltage and follow the field lines of the surrounding solenoid magnets through a slot hole in the anode.

High Voltage

Using an available ceramic of the DESY linacs the high voltage is limited to about 50 kV. In order to reach the design value of 150 kV the gun is surrounded by an insulating material for which SF_6 gas is used. Since the laser light must not penetrate the SF_6 gas, because otherwise the glass surfaces of the windows would be etched, it travels in air inside a tube (see fig. 2). The HV feed through has also been improved. With these modifications, the high voltage was limited by sparking in the vacuum chamber. This was improved by increasing the distance between anode and cathode and installing an additional ion sputter pump (400 l/s). Finally the voltage has been raised to 130 kV. However at the required magnetic field strength ($\sim$ 0.2T) the maximum value is reduced to about 80 kV. Some possible explanations could be a surface current on the glass prism or Penning effect.

Current

The peak current measured with a gap monitor was about 15 A at 50 kV. This is one order of magnitude lower than the expected value for a space charge limited current. If the limitation of the current is not due to space charge it can be enhanced by increasing the laser power density at the cathode surface. However, it may also be possible that it is limited by space charge or parts of the beam are lost by mechanical obstacles. In the next step an anode with a wider ring slot will be used.

Pulse Length

The laser produces a light pulse of about 10 ns total length. The main intensity is concentrated in about 3 ns; the two side maxima contain less then 10% of the light intensity. This profile was measured with a fast vacuum photo diode. The current response lasts about 9 ns (FWHM), measured with a gap monitor.

Azimuthal Homogeneity of the Ring Beam

It is important that the azimuthal charge distribution in the ring be as homogeneous as possible. Any inhomogeneity causes transverse wake fields which lead to transverse instabilities of the inner beam. However it seems very difficult to create a homogeneous electron ring beam.

Fig.4 shows the upper and lower part of the electron ring detected by the two cameras on the movable le fluorescent screen monitor. Until now two tantalum cathodes have been tested.

Several causes are considered for this inhomogeneity, e.g. an asymmetry in the laser profile or in the light path, a surface effect of the cathode or a mechanical obstacle for the electrons. The laser profile has been measured (see fig. 3) and it seems not to be the main cause for the inhomogeneity.

The four tags holding the inner part of the anode cause holes in the hollow beam (see fig. 4). However these holes do not effect the inner beam very much due to their fourfold symmetry.

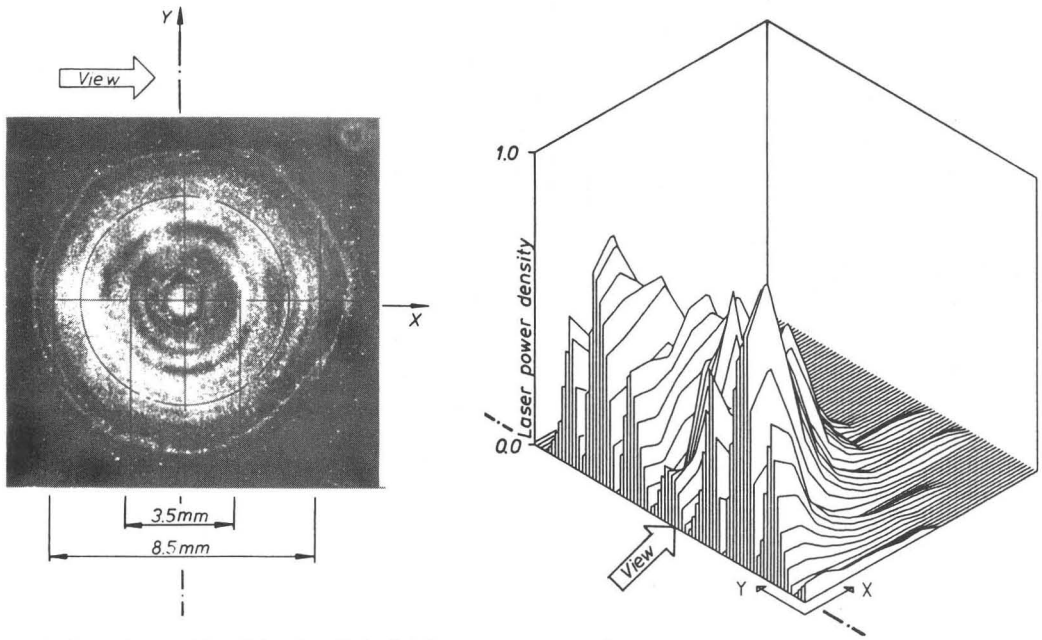

Fig. 3. *Spatial intensity profile of the Q-switched Nd-Yag laser beam ($\lambda = 1.064\,\mu m$). On the left side the profile is recorded on a "burn paper" and on the right side the profile is scanned with a pin hole power meter. A burn paper is an exposed and developed black and white photo paper. A single shot evaporates the silver coating on the paper proportional to the laser power density. This pattern gives a first impression of the spatial intensity profile. A pin hole power meter is a calorimeter where the sensitive area is reduced by a pin hole (here with a diameter of 1mm). The plot shows a vertical center cut through the profile. In both pictures a diffraction pattern is seen which is typical for this laser.*

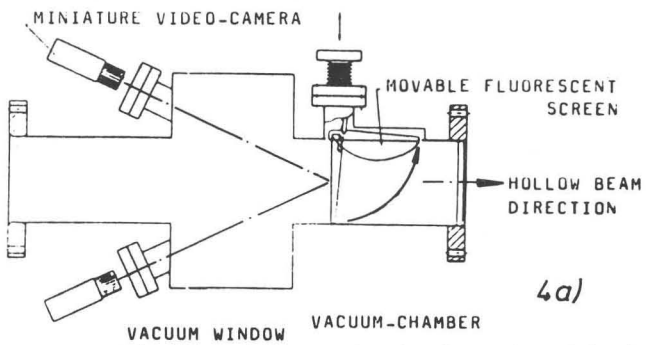

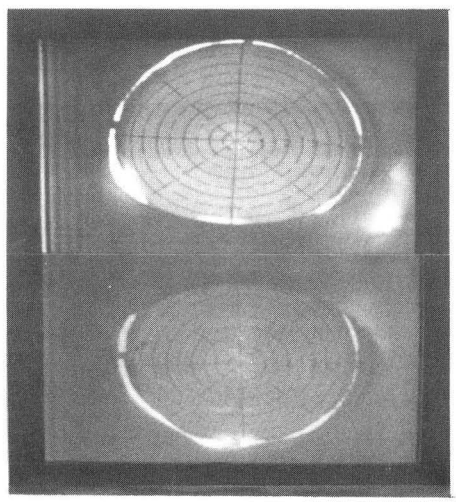

Fig. 4. *(a) Movable screen monitor for observation of the ring beam before acceleration (left at the top). (b) The electron ring beam hitting on a flourescent screen monitor after bunching seen by television cameras, upper part of the picture from below, lower from above (right at the top).*

THE LINAC

Prebuncher Cavity

So far, the prebuncher cavity has concentrated a low current electron beam to 5 short bunches of about 3 cm length each. With higher currents (higher laser power) the bunches are longer. This is interpreted as a space charge effect.

The prebuncher and the accelarating cavities are powered by one klystron which is pulsed at $25Hz$ with $100\mu s$ duration. As the buncher cavity is located in the magnetic field of the solenoid, multipactoring is much more severe than usual. The field strength breaks down after about $20\mu s$. Thus stable conditions cannot be achieved easily. In order to avoid this instability, the laser is triggered in the first rise before multipactoring takes place, about $10\mu s$ after the rf has been turned on. Due to filling time ($\approx 20\mu s$), however, at this point of time the rf level in the accelarating cavities has reached only a small fraction of its final value, so that no proper acceleration of the electrons takes place. Thus a separate rf amplifier for the prebuncher cavity, that can be triggered separately, is being installed, so that we can use the first stable region.

Accelerating Cavities

In the four 3-cell cavities the electrons are accelerated to about 6 MeV. A first phase shifter between the prebuncher cavity and the first accelerating cavity adjusts the injection phase. A second phase shifter between the first and the second cavity corrects for the delay in phase of the not yet relativistic electrons. The third phase shifter at the fourth cavity allows a variable energy spread for the high energy bunching in the antisolenoid.

Correction Coils

The movable screen in the low energy part and a fixed, but transparent fluorescent grid at the end of the linac allow the observation of the

position of the hollow beam, its actual diameter, its radial thickness and the azimuthal charge distribution.

We found a tendency of the ring to be slightly oval instead of round. This is caused by aberrations from the cylindrical symmetry of the solenoid coils and can be corrected by quadrupole correction coils. With two pairs of correction coils behind the first screen monitor a superposition of a dipole and quadrupole magnetic field can be produced, by adjusting the currents in the four coils individually. Thus both the shape and the position of the hollow be can be controlled.

BEAM DIAGNOSTICS

In the drift space of the prebuncher, a gap monitor and a movable fluorescent screen monitor were installed. For beam diagnostics after the acceleration a Čerenkov monitor, a gap monitor, a fluorescent grid and a special hollow beam spectrometer were added.

Gap Monitors

For the current measurement of the long bunches, gap monitors are used which simply interrupt the beam pipe by a ceramic ring. The image current on the wall induced by the beam current flows through some resistors bridging the gap (fig 6). The voltage signals appearing across these resistors are picked up. They contain information about the charge distribution longtudinally and transversly.

The first gap monitor in the low energy part consists of 64 resistors, 10Ω each. Sixteen 50Ω cables pick up the signals over an additional 50Ω resistor avoiding the reflection of backwards running signals. Eight of the 16 signals are summed up and can be observed either after a long cable with an oscilloscope or directly near the monitor with a sampling head to avoid damping and distortion of the signal.

Figure 5 shows two of five bunches separated by 2 ns. The oscillation of about 3 GHz is caused by a resonant circuit consisting of the capacity of the ceramic ring ($C \approx 50pF$) and the inductivity of the resistors and their connections ($L \approx 50pH$). This LC resonant circuit is damped by the low resistance of the 64 gap resistors (together 0.156Ω). Thus the signals produced by short bunches are hidden by oscillations. Fortunately longer bunches do not excite oscillations with such large amplitudes and thus can be observed reasonably well.

In the gap monitor at the end of the linac very short bunches would excite large oscillations. Therefore here the ohmic load is adjusted to aperiodic damping ($R = 1.56\Omega$) in order to get fast signal response while the oscillations are damped sufficiently. This is achieved without any resistors but only by bridging the gap with 32 pickup coax cables of 50Ω impedance.

If the ring beam is centered to the axis of the beam pipe the azimuthal charge distribution can be determined from the different amplitudes of the signals around the pipe. On the other hand the absolute value of the total beam is obtained by summing all the

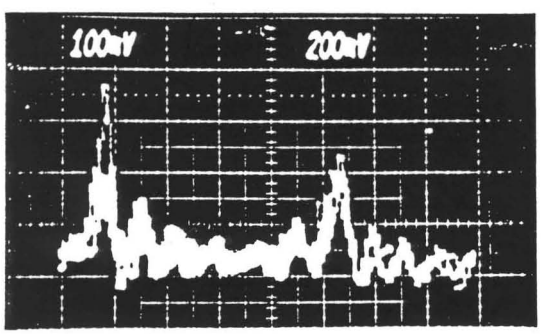

Fig. 5. *Two of 5 bunches produced by a single laser shot. The separation between them is 2 ns. The bunch length is about 150 ps (FWHM). The signals are produced by a gap monitor in front of the linac behind a drift space of 1.2 m after the end of the prebuncher cavity. They are detected by a sampling oscilloscope.*

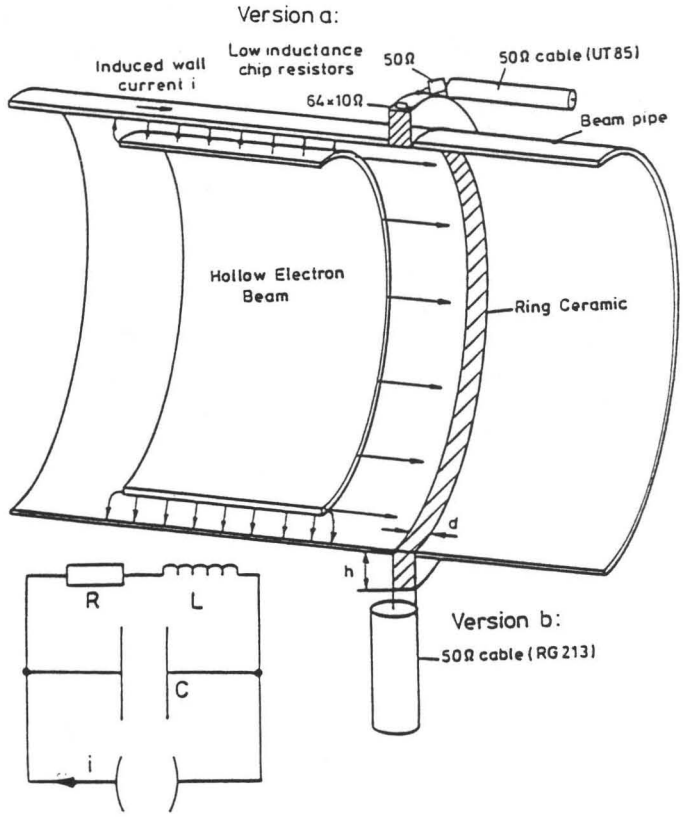

Fig. 6. *Physical layout and wiring of the gap monitor at the low energy end of the linac (Version a) and its equivalent circuit ($L = 50pH$, $C = 50pF$ and $R = 0.156\Omega$), which can explain the observed oscillations of about 3GHz between the bunches (see fig. 5). (Version b) Short conection from the ceramic ($d = 4mm$, $h = 7mm$) to one of the 32 big 50Ω cables damping the oscillations occuring at the high energy end aperiodically.*

pickups. This yields a signal which is approximatelly independent of the azimuthal beam distribution. Those signals have been compared with current measurements performed using a pulse transformer on the high voltage line feeding the cathode. Also here short pulses (10 ns) excite oscillations so that higher amplitudes are simulated. However the corrected values are consistent with the measurements of the gap monitors. The summed signals of the peak current derived from the both gap monitors agree within 15 % .

Čerenkov Monitor

To measure the length of short bunches (≤ 5 cm), the time resolution of 150 ps of the gap monitors is not sufficient. In order to resolve the expected bunch length of less than 1 cm properly, a time resolution of about 10 ps is necessary. This resolution can be achieved by a commercial streak camera (see fig. 7). The light pulse is created by the Čerenkov effect in glass. A similar arrangement has recently been used at slac [11]. A small part of the ring beam penetrates a quartz wedge and excites Čerenkov radiation. This light is then guided out by total reflections and leaves the beam pipe nearly perpendicular to the beam axis. An optical system (see fig. 8), consisting of 3 lenses and 2 mirrors, guides the light over 5 m to the streak camera, which is located far from the disturbing solenoid end field.

Fig.9 shows the streak camera signal of a bunch with 1 cm FWHM. So far, such short bunches can be achieved only at low current.

Hollow Beam Spectrometer

In order to analyze the energy of the hollow beam, a special hollow beam spectrometer (see fig. 10) has been developed. In the present stage, it is mounted at the end of the linac.

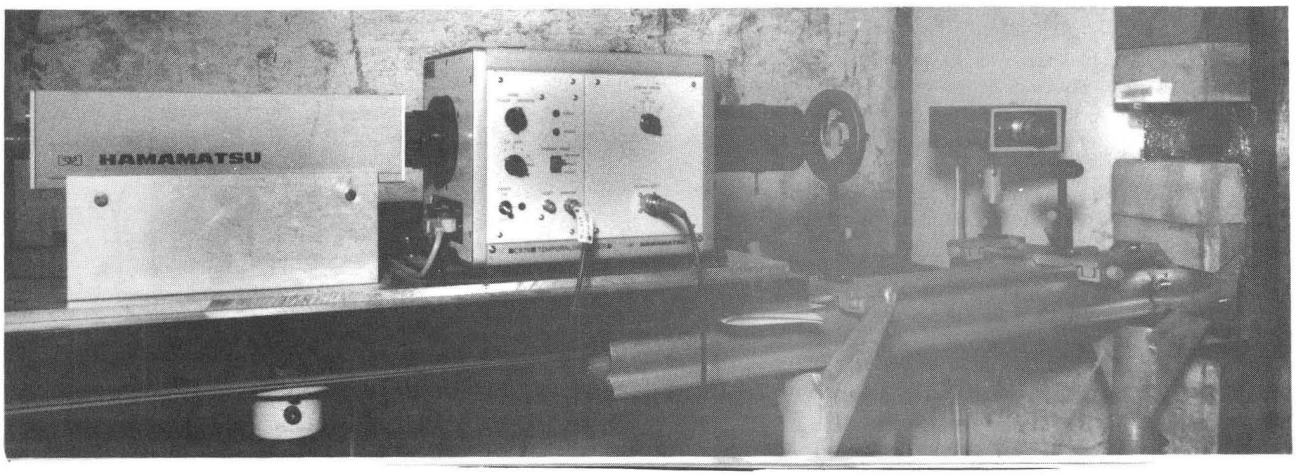

Fig. 7. *Streak camera: The Cerenkov light beam emerging from the pipe seen on the right side of the picture is focussed to the entrance split of the time disperser (middle part of the picture). The light signals scanned by the electron beam in the time disperser are recorded on a flourescent screen inside and are monitored by a television camera at the far left.*

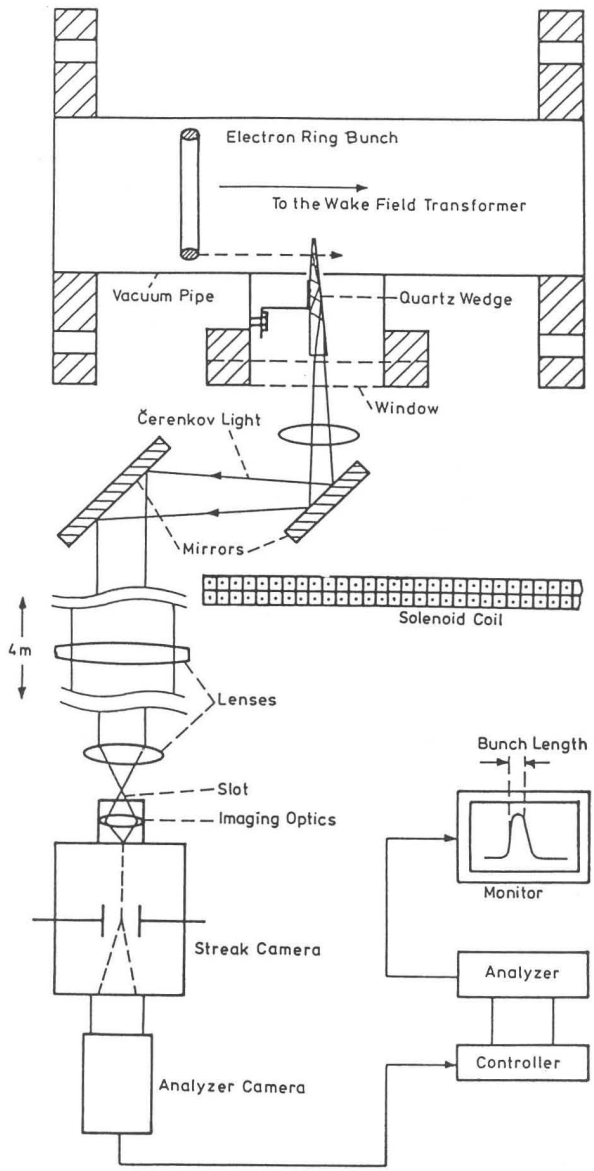

Fig. 8. *Setup of the Čerenkov light monitor for high resolution longitudinal beam size measurement of the hollow beam.*

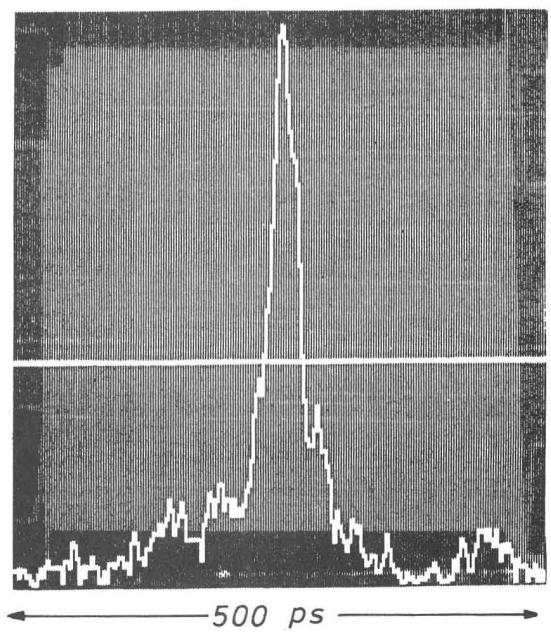

Fig. 9. *Single bunch signal taken with the streak camera. The width (FWHM) corresponds to a length of 1 cm.*

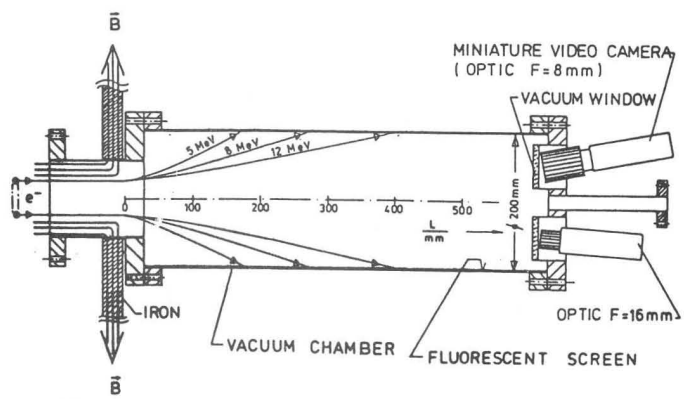

Fig. 10. *Hollow beam spectrometer making use of the end field of the solenoid on the left side (not shown). By an iron sheet (3 cm thick) the inner longitudinal field is bent outwards within a short range. Here the passing electrons experience a transverse momentum and hit the fluorescent screen at the inner wall of the spectrometer tube at a longitudinal position corresponding to their energy.*

In the short solenoid end field the particles experience an azimuthal kick and thus change their azimuthal velocity by $\Delta v_\phi = (erB)/(2\gamma m_0)$ (v_ϕ: azimuthal velocity after crossing the end field, γm_0: energy, r: radius, B: solenoid field strength). Particles of different energies hit a surrounding fluorescent pipe at different longitudinal positions. The flourescent light is observed by two television cameras viewing from the end of the pipe. From the longitudinal position, v_ϕ can be calculated and thus, knowing B and measuring r with a screen monitor, we can determine the energy.

For several reasons (space charge, transverse electric field components in the cavities, gaps between the solenoids) the electrons experience transverse forces and therefore oscillate around the lines of the guiding magnetic field. Presently it is not possible to determine the initial transverse velocity due to these effects when the electrons enter the end field at the spectrometer. This leads to an uncertainty in the energy measurement. In order to improve the accuracy a longitudinally movable screen has been installed by which the transverse electron velocity can be determined just before the spectrometer.

Furthermore, according to calculations, the oscillations can be suppressed by proper adjustment of the solenoid currents. Thus the movable screen will also be used in order to monitor appropriate adjustments.

COMPUTER SIMULATION

The computer code WAKTRACK has been extended to take space charge into account. Furthermore external data for cavity fields obtained from numerical solutions (URMEL) of Maxwell equations may be handled and wake field effects can be included (TBCI). Static electric and magnetic fields as calculated by the codes PROFI and MAFIA are also accepted and processed by WAKTRACK. [12].

Fig. 11 shows a typical plot output. In the lower part, the ring radius is plotted versus the longitudinal position of the ring along the linac. Above this curve the cavities with their phases and the positions of the solenoid coils are drawn.

In the upper part of the figure, the energy is drawn, in the low energy range, the difference to $\gamma = 1$ is stretched by a factor of 30. In the same part of the plot, the phase difference compared to a particle moving with the speed of light is shown.

Linac

For the tracking, initially a number of particles are assumed to be distributed on a ring, all having an energy of 75 keV.

The bunching effect of the prebuncher and the acceleration in each cavity cell can be observed.

Oscillations of the electrons around the magnetic field lines are excited by the radial cavity fields and radial magnetic field components, which occur at the gaps between the coils. By varying the current in some of the coils, the collective oscillation can be suppressed. However at the transition of the particles into the antisolenoid of the high energy buncher additional oscillations are excited due to the finite length of solenoid end fields. Investigations have been started to develop hollow beam focusing systems to counteract this effect and other non-collective effects such as radial space charge.

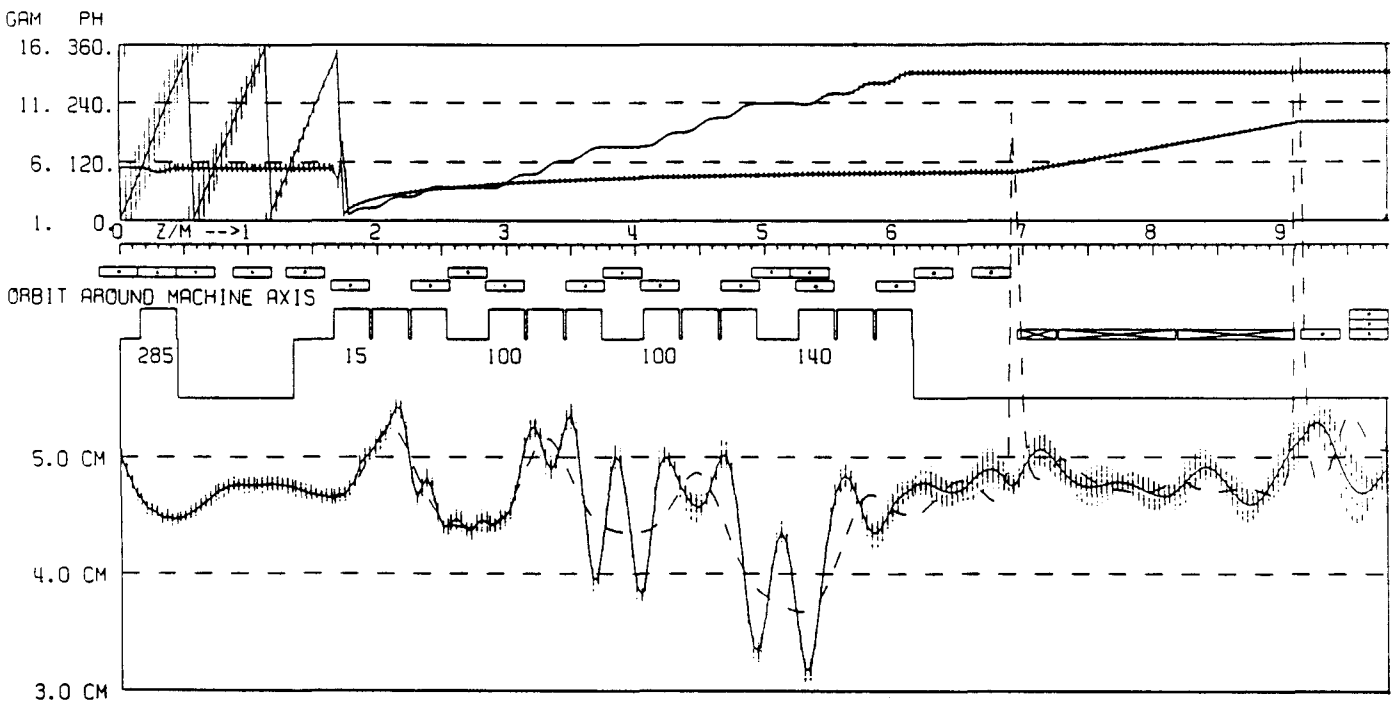

Fig. 11. *Typical plot output of the WAKTRACK tracking code, showing several particle properties in the DESY experiment. In the middle between the two frames, a scheme of the experimental set up is drawn, together with a scale, which can be compared to figure 1. The coils are sketched and near the cavity contours their phases are written in degrees. Below this, the orbit of the particles is plotted: the ring radius varies between 3 and 5 cm due to transverse forces at gaps between coils and in cavities. The collective oscillation around the dashed reference orbit is reduced in its amplitude by adjusting the current in the coils between the third and the fourth cavity (4.6 m < z < 5.6 m). Above the set up sketch two curves are plotted in one frame, the relativistic γ factor and the phase difference compared to a particle moving with the speed of light. In front of the first accelerating cavity (z < 1.7 m), where the particles are nonrelativistic, (γ − 1) is stretched by a factor of 30. Behind that, the increasing energy in the linac can be seen. The phase difference of nonrelativistic particles changes with a certain slope depending on the particle velocity. When the particle speed approaches c, the phase becomes constant. It only changes again in the high energy buncher (7 m < z < 9 m), where the velocity parallel to the z-axes is decreased by rotating the hollow beam.*

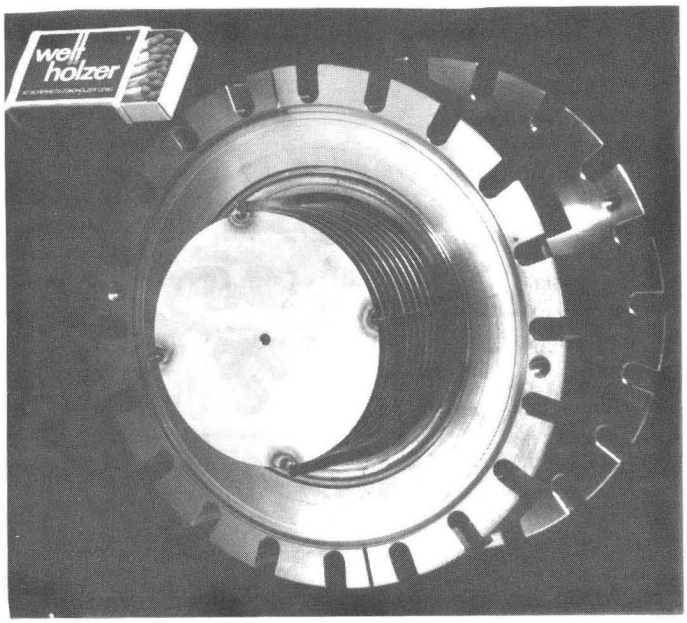

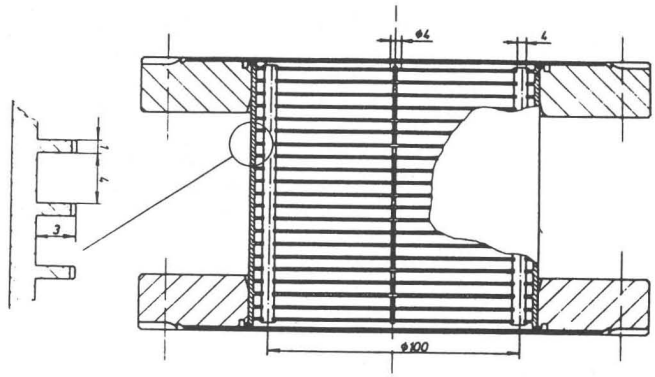

Fig. 12. *Wake field transformer: (a) The photo displays slices which are held together by metal strips forming a stack lying normally inside the tube. On the inner wall of this tube are ring shaped channels in which the wake fields are excited by the driving hollow beam. The wake fields are guided by the slices into the center of the tube where they interact with the driven beam. All parts are made from stainless steel. (b) Sectional drawing of a part of the wake field transformer.*

High energy buncher

The final longitudinal compression of the hollow beam is achieved in an antisolenoid. The field strength of the solenoid and of the antisolenoid are equal, the region where the field is radial must be very short. Therefore iron plates are inserted between the coils. The resulting field has been calculated with PROFI and included to the tracking code.

When the ring passes the radial field, the particles experience an azimuthal kick, which is just twice the kick of a solenoid end field. Thus the path of one particle in the antisolenoid is a spiral on a cylinder that has the same diameter as the ring beam, i.e. the ring is rotating, the radius does not change (see fig. 11). As some of the energy goes into the circular motion, the longitudinal velocity decreases i.e. the phase changes. The phase of the fourth cavity is adjusted such that the earlier particles are accelerated less than the later ones. Thus the ring can be bunched even at high energies, where classical rf bunching mechanisms fail.

At the end of the antisolenoid, the rotation is stopped by an inverse kick.

Wake Field Transformer

The first model built of the transformer is shown in fig. 12. For preliminary investigations independent of the available current we intend to create a low energy (50 keV) test beam just in front of the transformer. With this set up it will be possible to detect even small accelerating gradients due to the Wake Field Transformation. Of course 50 keV electrons will not be captured and accelerated optimally as they are nonrelativistic. However computer simulations show that a significant change in energy can be expected.

SUMMARY

So far we have studied the production and acceleration of the hollow beam for the Wake Field Transformer experiment. The gun will need some improvements in order to reach its design values. Screen monitors, gap monitors and the hollow beam spectrometer have been installed. The time resolution of the Čerenkov monitor is sufficient even for the short bunches which are expected at the end of the high energy buncher.

ACKNOWLEDGEMENT

The authors wish to thank all the DESY staff for their help.

References

[1] G.A.Voss and Th.Weiland, "Particle Acceleration by Wake Fields", DESY M-82-10, April 1982.

[2] G.A.Voss and Th. Weiland, "Wake Field Acceleration Mechanism", Proceedings of the ECFA Conference "The Challenge of Ultra High Energies", Oxford September 1982.

[3] Th. Weiland and F.Willeke, "Particle Tracking with Collective Effects in Wake Field Accelerators" Proceedings of the 12-th International Conference on High Energy Accelerators,Chicago, 1983, pp. 457-459 and following improved versions by Gary Rodens (Los Alamos) and Kaoru Yokoya (on leave from KEK).

[4] SLC-design report, SLAC report 229, June 1980.

[5] H. Piel, Recent Progress in RF Superconductivity, IEEE-NS-32(1985), page 3565.

[6] Proceedings of the Workshop on Laser Acceleration of Particles, AIP Conf. Proc. 91 , 1982.

[7] "The Challenge of Ultra-High Energies", Proceedings of the ECFA-RAL Workshop, Oxford, September 1982 ECFA 83/68.

[8] "The Generation of High Fields for Particle Acceleration to Very High Energies" Proceedings of the CAS-ECFA-INFN Workshop, Frascati, September 1984 ECFA 85/91 CERN 85-07 June 1985.

[9] W.Bialowons, H.Dehne, A.Febel, M.Leneke, H.Musfeldt, J.Rossbach, R.Rossmanith, G.A.Voss, Th.Weiland, F.Willeke, "A Wake Field Transformer Experiment" Proceedings of the 12-th International Conference on High Energy Accelerators, Chicago, 1983.

[10] W.Bialowons, H.D.Bremer, F.J.Decker, R.Klatt, H.C.Lewin, S.Ohsawa, G.A.Voss, Th.Weiland, "Wake Field Work at DESY", IEEE Transactions on Nuclear Science, Vol. NS 32-5,2 (1985), p.3471-3475

[11] J.C. Sheppard et al., "Real Time Bunch Length Measurements in the SLC Linac", SLAC-PUB-3584, February 1985.

[12] T.Weiland, On the numerical solution of Maxwell's equations and applications in the field of accelerator physics , Particle Accelerators 15 (1984) , 245-292 and references therein.